Introduction

The crosscorrelation (CC) of two recordings of seismic noise leads to an estimate of the Green's function between these two positions, as if one of them were an impulsive source. This method, called seismic interferometry (SI) has been successfully applied in seismology to retrieve surface waves using coda waves (Snieder, 2004) or using ambient-noise recordings. Besides surface waves, body waves can also be retrieved by ambient-noise SI in exploration seismics (Draganov *et al*., 2013). Active noise with known locations, such as drill-bit noise, has long been used in seismic-while-driling (SWD) to obtain reverse vertical seismic profiles (RVSP) (Rector and Marion, 1991, Poletto and Miranda, 2004). Most methods in SWD rely on pilot signals (estimates of the seismic signature of the drill-bit) to compress the drill-bit signal to an impulse (Poletto *et al*., 2014). The standard SWD processing involves crosscorrelating pilot signals and geophone recordings, reference deconvolution and pilot-delay shift. To apply SI to drill-bit data, Vasconcelos and Snieder (2008) used deconvolution SI and showed both numerical and field examples of using the retrieved reflections for imaging without pilot signals. Poletto *et al.* (2010) compared the method of drill-bit SI with and without pilot signals and showed field-data results from CC and deconvolution SI.

As the drill-bit is already in the subsurface and is closer to the target than receivers at the surface, an inter-source type SI (Curtis *et al.*, 2009) can also be useful to create virtual receivers from the drill-bit noise. However, previous applications of this type of SI assume that the source time functions are similar. To investigate the application of inter-source SI using non-transient source, such as drill-bit noise, we use synthetic drill-bit data from drilling noise in a horizontal well to retrieve virtual reflection responses at drill-bit positions. Practicalities of drill-string multiples and pilot delay shift are not included. We first look at the basic equations of inter-source SI by CC, and then show the numerical results. A migration image below the well using the retrieved reflection responses is compared with a surface-seismic image to show the potential advantage of using inter-source SI with drill-bit data.

Method

Applying source-receiver reciprocity to the conventional inter-receiver type SI by CC (Wapenaar and Fokkema, 2006) gives an inter-source type of SI (Curtis *et al.*, 2009), which reads

$$G(\mathbf{x}_A\,|\,\mathbf{x}_B)+G^*(\mathbf{x}_A\,|\,\mathbf{x}_B)\propto\oint_{\partial D}G^*(\mathbf{x}\,|\,\mathbf{x}_A)G(\mathbf{x}\,|\,\mathbf{x}_B)d\mathbf{x}. \qquad (1)$$

Here, the Green's function $G(\mathbf{x}_A\,|\,\mathbf{x}_B)$ represents the acoustic wavefield observed at $\mathbf{x}_A$ due to an impulsive point source at $\mathbf{x}_B$. Upper-case symbols represent quantities in the frequency domain. The superscript * denotes complex conjugate. It can be interpreted that instead of the Green's function between two receivers, the CC of the response at $\mathbf{x}$ due to the impulsive point sources at $\mathbf{x}_A$ and at $\mathbf{x}_B$, and the subsequent summation of the correlated responses over all receiver positions, retrieves the estimated Green's function between two sources. For drill-bit data, an impulsive point source is replaced by the drill-bit source function $s(t)$, and we write the observed response at $\mathbf{x}$ due to the source at $\mathbf{x}_i$ (i can be A or B) as

$$Y(\mathbf{x}\,|\,\mathbf{x}_i)=G(\mathbf{x}\,|\,\mathbf{x}_i)S(\mathbf{x}_i)\,. \qquad (2)$$

Then following Eq.1, the CC of the recordings at $\mathbf{x}$ due to the source at $\mathbf{x}_A$ and $\mathbf{x}_B$ gives

$$\begin{aligned}\int_{\partial D_0}Y^*(\mathbf{x}\,|\,\mathbf{x}_A)Y(\mathbf{x}\,|\,\mathbf{x}_B)d\mathbf{x}&=S^*(\mathbf{x}_A)S(\mathbf{x}_B)\int_{\partial D_0}G^*(\mathbf{x}\,|\,\mathbf{x}_A)G(\mathbf{x}\,|\,\mathbf{x}_B)d\mathbf{x}\\&\propto S^*(\mathbf{x}_A)S(\mathbf{x}_B)(G(\mathbf{x}_A\,|\,\mathbf{x}_B)+G^*(\mathbf{x}_A\,|\,\mathbf{x}_B)).\end{aligned} \qquad (3)$$

Here, the surface boundary ∂D is replaced by ∂D_0, which denotes the receiver surface. Given a wide and sufficient coverage of receivers, this substitution is possible because the stationary-phase positions for retrieving the reflections from below the drill-bit lie mainly at the surface. Now we have $S^*(\mathbf{x}_A)S(\mathbf{x}_B)$ on the right-hand side and when the drill-bit signals are different, it has a random phase and therefore changes the phase of the retrieved Green's function on the right-hand side. This does not happen for inter-receiver SI, because it is always the CC of the responses from the same source. As the drill-bit source function varies, it requires the estimates of the source signals to be known in order to apply inter-source SI. For drill-bit SI, this means applying standard SWD processing using pilot signals before applying SI. Here we describe such drill-bit signal deconvolution as

$$\widetilde{G}(\mathbf{x}\,|\,\mathbf{x}_A) = \frac{Y(\mathbf{x}\,|\,\mathbf{x}_A)\widetilde{S}^*(\mathbf{x}_A)}{|\widetilde{S}(\mathbf{x}_A)|^2}, \qquad (4)$$

where $\tilde{S}(\mathbf{x}_A)$ is the pilot signal of the drill-bit at $\mathbf{x}_A$ and $\widetilde{G}(\mathbf{x}\,|\,\mathbf{x}_A)$ represents the estimated impulse response from the drill-bit to the receiver. Then one can use Eq.1 to estimate the Green's function between sources. Therefore, unlike inter-receiver SI using noise sources, the phase of reflections between sources (non-zero offset) can only be retrieved by SI without any information of the source signal, when the source signals are the same.

Synthetic drill-bit noise example

We demonstrate the method using synthetic drill-bit data to retrieve the virtual response between drill-bit positions. The P-wave velocity model is shown in Fig.1. There are 121 receivers (denoted by triangles) at the surface with a spacing of 50 meters. We model 81 shots at the drill-bit positions (denoted by stars) with a spacing of 25 meters using a Ricker wavelet, and then convolve with different drill-bit source functions to create the synthetic drill-bit data. Fig.2 a) shows the modelled drill-bit source function $s(t)$ at $x = 3000$ m and panel b) shows the pilot signal $\tilde{s}(t)$ with about 5% noise. The noise is shown in panel c). Fig.3 a) shows a raw common-source gather at $x = 3000$ m, while panels b) and c) show the pilot-deconvolved common-source gathers using $s(t)$ and $\tilde{s}(t)$, respectively. The retrieved responses using inter-source SI by CC (Eq.1) are shown in Fig.4. Energy normalization is applied after the interferometry process for panel b) and d), which use the noise-contaminated pilot signal $\tilde{s}(t)$. No energy normalization is applied for panel a) and c), which use the exact source signal $s(t)$. Using the above procedure, we retrieve common-source gathers for a source at each drill-bit position and virtual receivers at all other drill-bit positions. Then we migrate the retrieved responses from the pilot-deconvolved data using standard prestack depth migration with a simple homogeneous velocity of 2750 m/s (2500 m/s +10% error). The result is shown in Fig. 5 a). Note that the velocity in the layer where the drill-bit positions are situated is 2500 m/s and the velocities of the two layers below it are 3300 m/s and 4000 m/s, respectively. Fig. 5 b) shows an image of the subsurface reflectors obtained from the surface seismic reflection data using the 10-percent erroneous migration velocity. We can see that the deep reflectors are mispositioned more severely in Fig. 5 b) than in Fig. 5 a).

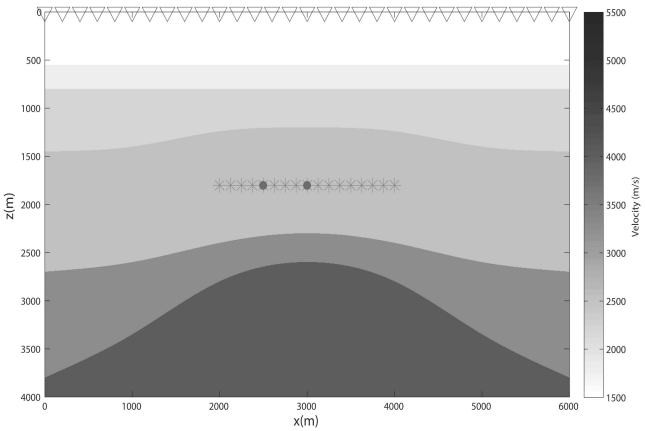

Figure 1 *The P-wave velocity model. Triangle denotes receiver and star denotes drill-bit source position. The two solid circles indicate the reference positions. Every fifth source and receiver are plotted.*

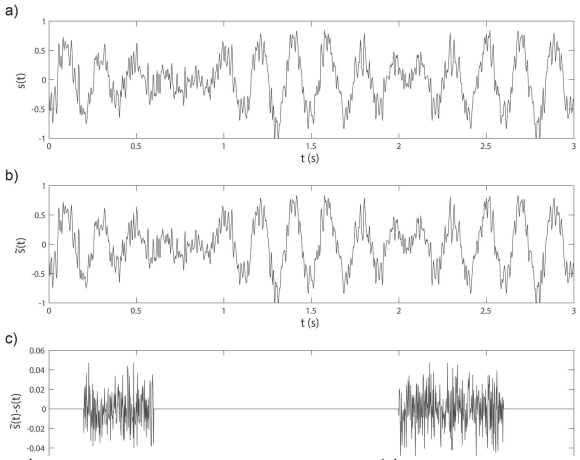

Figure 2 *Modelled drill-bit signal. a) The exact drill-bit source function* $s(t)$. *b) The pilot signal* $\tilde{s}(t)$. *c) The noise applied to the pilot signal, which is up to 5% of the exact drill-bit signal.*

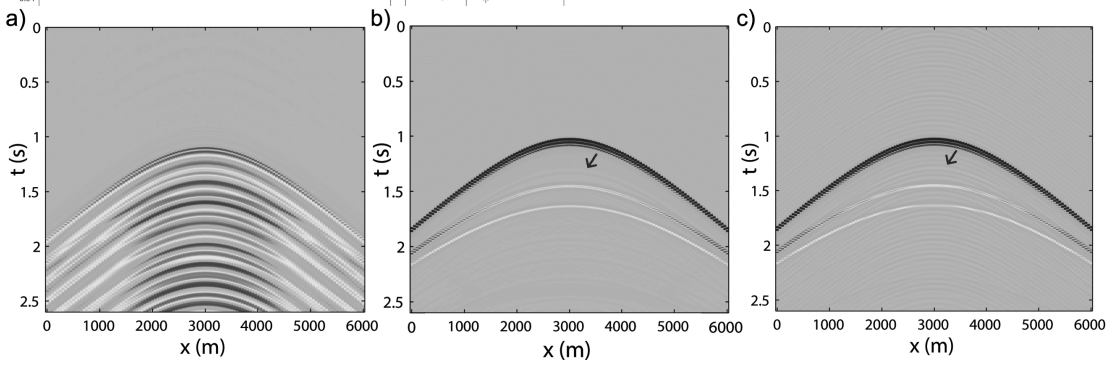

Figure 3 *Modelled common-source gather and pilot-deconvolved results. a) Raw common-source gather from drilling noise at* $x = 3000\,m$. *Pilot-deconvolved common-source gathers using b) the exact source signal* $s(t)$ *and c) the noise-contaminated pilot signal* $\tilde{s}(t)$. *The arrow indicates the internal multiple from the second layer, which arrives about 0.2 seconds after the direct waves.*

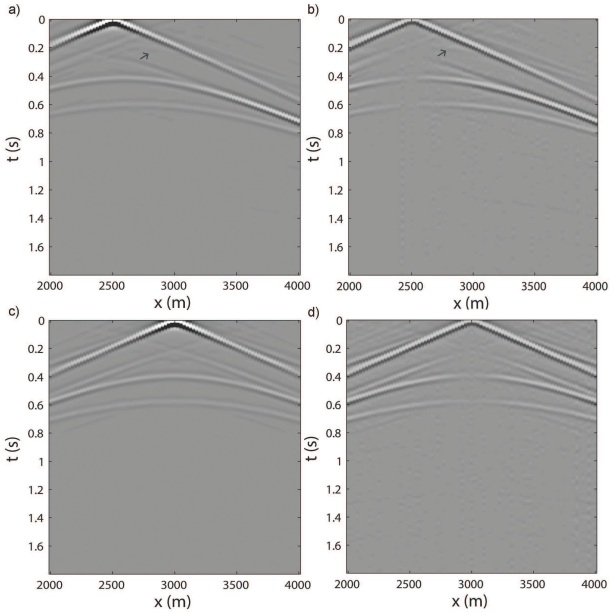

Figure 4 *Retrieved common-source response at the drill-bit positions. The top row corresponds to the virtual drill-bit receiver data from a virtual source at* $x = 2500\,m$ *and the bottom row from a virtual source at* $x = 3000\,m$. *a) and c) are retrieved after using the exact drill-bit source function for pilot deconvolution, and b) and d) after using* $\tilde{s}(t)$ *for pilot deconvolution and applying energy normalization to the retrieved response. The arrows indicate the non-physical reflections identified as the CC of the direct waves and the internal multiples.*

Discussion and conclusion

From the above results, it is clear that the information about the drill-bit noise is essential for the retrieval of the virtual response between the drill-bit positions. In practical applications, the useful signal from the pilot at the drill-bit should have sufficient signal-to-noise ratio. When the level of the interfering noise (e.g. from the noise inside the borehole) is too high, the method might not work. The method we propose will work best with receivers that can be left in the field for the time of the drilling. This means that the method's natural area of application would be with receiver arrays on land or with ocean-bottom stations or cables. In all three cases, the receiver spacing should not allow aliasing of the recorded wavefields. Note that the length of the receiver array (extent of the network)

would dictate the positions of the drill-bit between which a reflection response can be retrieved. The two drill-bit positions and the receiver geometry must be such that the receivers cover the stationary-phase region for retrieval of reflections between the two drill-bit positions. The retrieved responses can be used for more accurate imaging of the deep area that is independent of the velocities of the overburden, as the retrieved virtual response have been interferometrically redatumed to the borehole level.

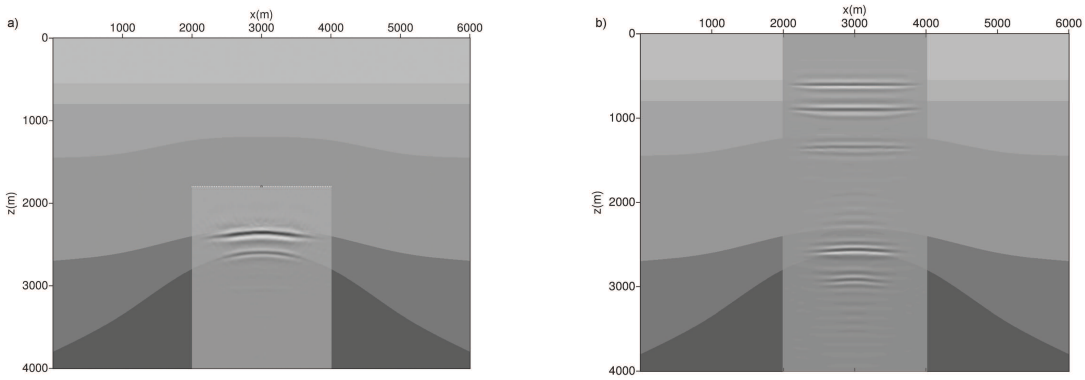

Figure 5 *Migration images a) using retrieved virtual reflection responses at the drill-bit positions, and b) using conventional surface seismic reflection data. The background indicates the true velocity model. Image a) is obtained using a homogeneous velocity model of 2750 m/s (2500 m/ +10% error), while image b) is obtained using the 10% higher velocities of the whole model.*

Acknowledgement

The authors acknowledge the Research Council of Norway, ConocoPhillips, Det norske oljeselskap, Statoil, Talisman, TOTAL and Wintershall for financing the work through the research centre DrillWell - Drilling and Well Centre for Improved Recovery, a research cooperation between IRIS, NTNU, SINTEF and UiS; and the ROSE consortium at NTNU. The research of D.D is supported by the Division for Earth and Life Sciences (ALW) with financial aid from the Netherlands Organization for Scientific Research (NWO) with VIDI grant 864.11.009.

References

Curtis, A., H. Nicolson, D. Halliday, J. Trampert, and B. Baptie. 2009. Virtual seismometers in the subsurface of the Earth from seismic interferometry. *Nature Geoscience* 2, 700 - 704.

Draganov, D., X. Campman, J. Thorbecke, A. Verdel, and K. Wapenaar. 2013. Seismic exploration-scale velocities and structure from ambient seismic noise (>1 Hz). *Journal of Geophysical Research: Solid Earth* 118, 4345 - 4360.

Snieder, R.. 2004. Extracting the Green's function from the correlation of coda waves: A derivation based on stationary phase. *Phys. Rev. E* 69, no. 4, 046610.

Poletto, F., and F. Miranda. 2004. *Seismic While Drilling: Fundamentals of Drill-Bit Seismic for Exploration*. Pergamon. 35.

Poletto, F., P. Corubolo, and P. Comelli. 2010. Drill-bit seismic interferometry with and without pilot signals. *Geophysical Prospecting* 58, 257-265.

Poletto, F., F. Miranda, P. Corubolo, A. Schleifer, and P. Comelli. 2014. Drill-bit seismic monitoring while drilling by downhole wired-pipe telemetry. *Geophysical Prospecting* 62, 702 - 718.

Rector, J., and B. Marion. 1991. The use of drill-bit energy as a downhole seismic source. *Geophysics* 56, 628 - 634.

Vasconcelos, I., and R. Snieder. 2008. Interferometry by deconvolution: Part 2 - Theory for elastic waves and application to drill-bit seismic imaging. *Geophysics* 73, S129 - S141.

Wapenaar, K., and J. Fokkema. 2006. Green’s function representations for seismic interferometry. *Geophysics* 71, SI33 - SI46.